

Article

# Performance Analysis of Full Duplex Bidirectional Machine Type Communication System Using IRS with Discrete Phase Shifter

Periyakarupan Gurusamy Sivabalan Velmurugan <sup>1</sup>, Sundarrajan Jayaraman Thiruvengadam <sup>1</sup>,  
Vinoth Babu Kumaravelu <sup>2,\*</sup>, Shrinithi Rajendran <sup>1</sup>, Roshini Parameswaran <sup>1</sup>  
and Agbotiname Lucky Imoize <sup>3,4,\*</sup>

<sup>1</sup> Department of ECE, Thiagarajar College of Engineering, Madurai 625015, India; pgsvels@tce.edu (P.G.S.V.);

<sup>2</sup> Department of Communication Engineering, School of Electronics Engineering, Vellore Institute of Technology, Vellore 632014, India

<sup>3</sup> Department of Electrical and Electronics Engineering, Faculty of Engineering, University of Lagos, Akoka, Lagos 100213, Nigeria

<sup>4</sup> Department of Electrical Engineering and Information Technology, Institute of Digital Communication, Ruhr University, 44801 Bochum, Germany

\* Correspondence: vinothbab@gmail.com (V.B.K.); aimoize@unilag.edu.ng (A.L.I.)

**Abstract:** In this paper, passive Intelligent Reflecting Surface (IRS) is used to enhance the performance of a Full Duplex (FD) bidirectional Machine Type Communication (MTC) system with two source nodes. Each node is equipped with two antennas to operate in FD mode. In reality, self-interference and discrete phase shifting are two major impairments in FD and IRS-assisted communication, respectively. The self-interference at source nodes operating in FD mode is mitigated by increasing the number of meta-surface elements at the IRS. Bit Error Rate (BER) and outage performances are analyzed with continuous phase shifting and discrete phase shifting in IRS. Closed-form analytical expressions are derived for the outage probability and BER performances of the IRS-assisted bidirectional FD-MTC system with a continuous phase shifter. The outage and BER performances of the IRS-assisted bidirectional MTC system in the FD mode have Signal-to-Noise Ratio (SNR) improvement compared with the IRS-assisted bidirectional MTC system in Half Duplex (HD) mode, as the number of reflecting elements in IRS is doubled in the FD mode. The outage and BER performances are degraded by a discrete phase shifter. Hence, performance degradation of the proposed IRS-assisted bidirectional FD-MTC is examined for 1-bit shifter ( $0, \pi$ ), 2-bit shifter ( $0, \pi/2, \pi, 3\pi/2$ ), and for 3-bit shifter ( $0, \pi/4, \pi/2, 3\pi/4, \pi, 5\pi/4, 3\pi/2, 7\pi/4$ ). The performance degradation when a discrete phase shifter is employed in IRS is compared with the ideal continuous phase shifter in IRS. Further, achievable rate analysis is carried out for finding the best location of the IRS in a bidirectional FD-MTC system.

**Keywords:** Intelligent Reflecting Surface; bidirectional; bit error rate; outage probability; discrete phase shifter; machine type communication



**Citation:** Velmurugan, P.G.S.; Thiruvengadam, S.J.; Kumaravelu, V.B.; Rajendran, S.; Parameswaran, R.; Imoize, A.L. Performance Analysis of Full Duplex Bidirectional Machine Type Communication System Using IRS with Discrete Phase Shifter. *Appl. Sci.* **2023**, *13*, 7128. <https://doi.org/10.3390/app13127128>

Academic Editor: Christos Bouras

Received: 17 May 2023

Revised: 8 June 2023

Accepted: 12 June 2023

Published: 14 June 2023



**Copyright:** © 2023 by the authors. Licensee MDPI, Basel, Switzerland. This article is an open access article distributed under the terms and conditions of the Creative Commons Attribution (CC BY) license (<https://creativecommons.org/licenses/by/4.0/>).

## 1. Introduction

Fifth-Generation (5G) wireless communication operating in the millimetre (mm) wave spectrum (30–300 GHz) is easily blocked or diffused by a physical object like buildings or atmospheric and environmental events [1,2]. The major challenge of data transfer using 5G is that it cannot carry data over longer distances. Intelligent Reflecting Surface (IRS) is the emerging paradigm for the next generation of wireless communication. IRS is a new type of radio environment that leverages smart radio surfaces, whose response can be adapted to the status of the propagation environment through control signaling [3]. It has the advantage of achieving high spectral and energy efficiency in wireless communications.

IRS is enabled by a metamaterial surface that can be electronically reconfigured to alter the propagation of radio waves. This reconfigurability of the radio environment in IRS overcomes many of the restrictions of conventional wireless communication, such as interference, shadowing, and multi-path propagation. IRS can be used in both indoor and outdoor environments of wireless communication systems, such as 5G and beyond 5G (B5G), to achieve better signal quality and coverage, and it can also be integrated with other wireless technologies, such as beamforming to achieve a more efficient wireless communication system.

Machine Type Communication (MTC) is specially designed with low power consumption, low data rate, and high reliability for Machine-to-Machine (M2M) and Internet of Things (IoT) applications [4]. MTC devices are typically embedded in everyday objects and communicate with other devices to perform specific tasks. Examples include smart meters, industrial automation systems, and connected vehicles. It involves the exchange of information between two or more machines, without the need for human intervention. On the other hand, MTC devices are designed to operate in harsh environments and must be able to function reliably in the presence of interference and noise. MTC connects machines wirelessly to form an interconnection of machine-type devices known as IoT. Even in large path loss, it can establish communication with unidirectional relaying or bidirectional relaying, which operates in Decode and Forward (DF) or Amplify and Forward (AF) mode [5]. In the proposed system, IRS is used in place of DF relaying to improve the channel gain between two machines. More meta surface elements are required in IRS to improve channel gain [6]. MTC operates in bidirectional FD mode for simultaneous transmission and reception of data over the same frequency band is considered in the proposed system model. Combining the benefits of IRS with MTC will improve the spectral efficiency and reliability of the bidirectional MTC communication system. When the smart radio environment capability of IRS is combined with the MTC system, it provides numerous applications in smart cities, industrial automation, healthcare, smart transportation, wireless sensor networks, the IoT, 5G, and B5G cellular networks. IRS-assisted MTC system is shown in Figure 1. To meet practical deployment difficulties, discrete phase shifters are considered at the IRS [7] in the proposed system model.

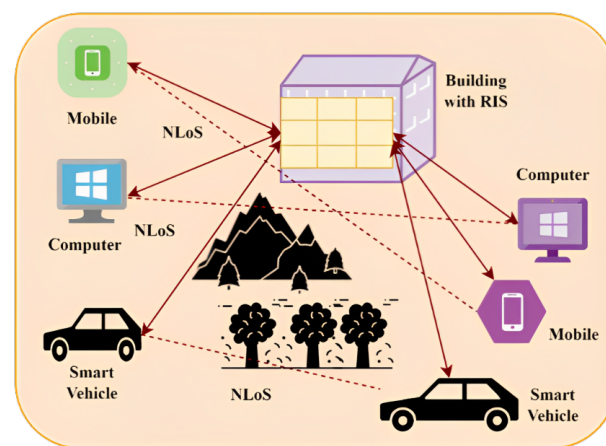


**Figure 1.** IRS-assisted MTC system.

#### *Related Work*

One of the most common use cases of 5G involves massive MTC, in which the machines communicate to one another directly over any communication channel [8]. The transition from 5G to Sixth-Generation (6G) will also hasten the transition from Industry 4.0 to Industry 5.0, where humans and machines collaborate safely and seamlessly [9]. Full industrial automation necessitates ultra-reliable, low-latency communications (URLLC). IRS could be one of the potential solutions to many of the smart manufacturing challenges. It has the potential to improve wireless network efficiency in terms of data rate and

connectivity. IRS can help smart manufacturing by providing services such as blockage mitigation, wireless power transfer, sensing and localization, edge computing, and so on.

The outage probability and ergodic capacity expressions for a bidirectional AF relaying system over Nakagami- $m$  fading are developed in [10] considering hardware constraints. An FD Simultaneous Transmission and Reflection (STAR)-IRS is proposed, in which the FD base station (BS) communicates with both uplink (UL) and downlink (DL) users over the same time-frequency [11]. The goal of this proposal is to reduce total transmit power while maintaining the minimum data rate requirement. The proposed system's performance is compared to that of conventional IRS and HD IRS systems. A similar system is proposed in [12], where the probability density functions (PDF) of UL and DL users are first derived. Using these, analytical closed-form outage probability and throughput expressions for both UL and DL users are derived. Monte Carlo (MC) simulations are used to validate the accuracy of derived expressions. The STAR-IRS-FD communication system outperforms the conventional IRS-aided system by 5% to 50%. An IRS-assisted FD communication system is suggested, in which the FD-BS communicates with both UL and DL users at the same time [13]. The analytical outage probability expressions for UL and DL are derived and verified via MC simulations. It has been established that systems with IRS perform better than systems without IRS. An IRS-mounted FD Unmanned Aerial Vehicle (UAV) with non-orthogonal multiple access is recommended to aid in the simultaneous transfer of information from the BS to all ground users [14]. Three different transmission modes are discussed here: FD-UAV aided, IRS-aided, and joint IRS-FD-UAV. The achievable sum rate of the network is maximized through optimization.

The energy efficiency of the STAR-IRS-FD system is maximized by optimizing the transmit power of the BS and UL users as well as passive beamforming at IRS [15]. To optimize power, Dinkelbach's method is used, whereas, for passive beamforming, the penalty-based method and successive convex approximation are used. The energy efficiency of an IRS-aided point-to-point system, where the transmitter and receiver are both outfitted with multiple antennas and operate in FD mode, is enhanced through joint beamforming at sources and IRS [16]. For optimization, the authors adopted a similar approach as employed in [15]. The suggested scheme's energy efficiency is demonstrated to be superior to the sum rate maximization scheme. This scheme can extend the life of communication devices without degrading their performance. The influence of sensing energy and data availability on the throughput performance of energy-harvesting cognitive radio networks (CRN) is discussed in [17]. The secondary network's transmitters are powered by the energy, harvested from primary users' radio frequency (RF) signals. The suggested approach has been tested in extreme cases of heavy and general data arrival. The authors of [18] investigated ambient backscatter (AB)-assisted RF-powered underlay CRN and its long-term secondary user throughput is optimized using two algorithms: adjusted-deep deterministic policy gradient (A-DDPG) and convex optimization assisted A-DDPG. Through simulations, it is demonstrated that these two methods outperform the conventional AB-aided overlay CRN and AB-aided underlay CRN. These CRNs do not use IRS in their communication chain.

IRS-assisted URLLC networks with nonlinear energy harvesting are proposed for industrial automation [19]. A remote data centre communicates with multiple machines via the FD server and IRS. The server is assumed to be nearer to the machines in this case. IRS facilitates the reception of signals by the server from data centers, while nonlinear energy harvesting techniques specifically tackle the problem of insufficient transmit power from the server. The end-to-end performance of FD-IRS is examined in this work by deriving expressions for Block Error Rate (BLER) for various scheduling algorithms. The performance of the suggested system is evaluated through the number of IRS elements, packet size, and different channel conditions. MC simulations are employed to validate the derived BLER expressions.

IRS is used in [20] to fill coverage gaps in multiuser cellular FD links while also suppressing self-interference (SI) and co-channel interference. This approach allows BS and all users to exchange information at the same time, potentially doubling spectral efficiency.

In this study, the BS precoding matrix and the IRS reflection coefficient are jointly optimized to maximize the minimum rate requirement of all users. In [21], active beamforming at sources and passive beamforming at IRS are jointly optimized to minimize total transmit power while maintaining minimum data rate requirements of sources. Semidefinite relaxation is used to obtain the active beamforming vectors. To solve the passive beamforming problem, successive convex approximation and semidefinite programming are used. Simulations show that the recommended FD-IRS achieves a higher performance gain than an IRS-assisted HD system. In [22], an IRS-aided IoT network operating in in-band FD mode is suggested. In this case, all IoT node pairs communicate at the same time and frequency via individual IBFD links. As a result, the nodes experience high SI and inter-node interference. Active beamforming at each node and passive beamforming at IRS are jointly optimized in this work to minimize total network transmit power while meeting the minimum rate requirement of each IoT node. The effect of IRS elements, nodes, and hardware flaws on system performance is also investigated. The performance of an IRS-aided multiuser FD secure communication system is examined in the presence of failures of the hardware at the transmitter, receiver, and IRS [23]. Deep reinforcement learning is employed for joint optimization at BS and IRS to maximize the sum secrecy rate. The IRS strengthens the secrecy against multiple eavesdroppers overhearing the two-way transmitted signals. The security vulnerabilities that could exist in a 6G communication network supported by IRS are described in [24]. In this work, meta-surface manipulation attacks which take place as a result of the manipulation of meta-surface behaviour are examined. In the context of Physical Layer security (PLS), two case studies involving information exploitation and information-gathering attacks are presented. These vulnerability cases are thoroughly investigated using BER and positive secrecy capacity metrics.

Three transmission modes, namely direct, relay-aided, and IRS-aided communication, are addressed in the device-to-device (D2D) communication network [25]. The switching between different transmission modes is performed dynamically based on the network conditions and the availability of relays and IRS. The authors propose a switching algorithm that determines the optimal transmission mode based on the distance between devices, the signal strength, and the availability of relays and IRS. In [26], D2D unidirectional communication performance is enhanced by an iterative optimization algorithm for several parameters of the system, such as transmit power, IRS passive transmit beamforming, and BS receive beamforming. The IRS-assisted D2D communication provides the advantage of improved Signal-to-Interference Noise Ratio (SINR) and extends the coverage area compared to traditional D2D communication [27].

Most conventional studies implement IRS reflection coefficients with continuous phase shifters, which is expensive and difficult to realize due to hardware limitations. It is more convenient to use IRS phase shifts with the finite resolution, which may reduce signaling overheads and energy consumption when acquiring instantaneous channels [28]. An analysis of the trade-off between spectral efficiency and energy efficiency in a multiuser multiple input multiple output (MIMO) UL system supported by IRS with discrete phase shifters is presented in [29]. To maximize resource efficiency, the precoding matrix at users and the beamforming matrix at IRS are optimized jointly. The discrete IRS phases are constructed employing an iterative mean square error minimization method [30]. The authors of [31] demonstrated that the difference in sum rate performance between a continuous phase shifter and a 1-bit discrete phase shifter is negligible. In [32], an IRS prototype at 28 GHz is realized using a two-bit discrete phase shifter. The analysis of the impact of discrete phase shifters on BER and outage performance would be more beneficial for design and practicing engineers in the field of 6G wireless communications [7]. Motivated by the above, in this paper, an IRS-assisted bidirectional FD-MTC system is proposed. In comparison with related works, this paper is the first to analyze the performance of the IRS-assisted bidirectional FD-MTC system.

The major outcomes of this paper are highlighted below:

- Analytical expression is derived for the outage probability and BER of the bidirectional FD-MTC system assisted by an ideal continuous phase shifter at IRS. The analytical derivations are confirmed by an MC simulation. The performance is also compared with the IRS-assisted bidirectional HD-MTC system.
- A detailed investigation on the outage and BER of the bidirectional FD-MTC system is carried out for non-ideal cases of the discrete phase shifter (1-bit, 2-bits, and 3-bits) at IRS.
- Further, the analysis is carried out for the achievable rate in various locations of the IRS in a bidirectional FD-MTC system to determine the optimal location of the IRS.

The paper is organized as follows: the system model of the proposed IRS-assisted bidirectional FD-MTC system is described in Section 2. The performance analysis of the proposed system in terms of outage probability, BER, and achievable rate is investigated in Section 3. In Section 4, the analytical results are verified using MATLAB simulation and we discuss the inference of the proposed system. Finally, Section 5 concludes this paper.

### 2. System Model

An IRS-assisted bidirectional FD-MTC system is shown in Figure 2, with two source nodes  $S_1$  and  $S_2$ . Each node is assumed to have two antennas. The Line of Sight (LoS) link is weak between the two nodes due to obstacles and fading. Hence, IRS is placed between the two source nodes  $S_1$  and  $S_2$  to enhance the data exchange between them. IRS is composed of  $N$  reflecting metasurface elements. FD mode is employed in the proposed bidirectional MTC system, for simultaneous transmission and reception. Due to FD operation mode, SI occurs at two source nodes  $S_1$  and  $S_2$ .

Binary Phase Shift Keying (BPSK) symbols  $x_1$  and  $x_2$  are transmitted by source nodes  $S_1$  and  $S_2$ , respectively. The transmit powers of both the source nodes  $S_1$  and  $S_2$  are assumed to be the same as  $P_s$ . The physical channels between the source nodes  $S_1, S_2$ , and the IRS follow independent and identical distribution (i.i.d) of Rayleigh fading with mean  $\sigma\sqrt{\pi/2}$  and variance  $((4 - \pi)/2)\sigma^2$ , where  $\sigma$  is the scale parameter of the distribution.

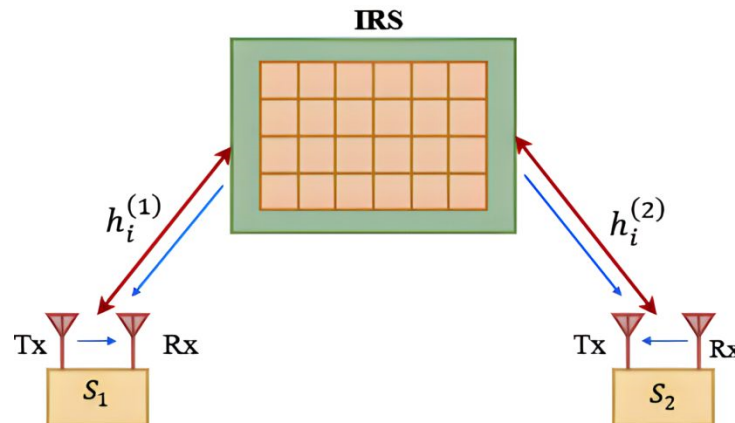


Figure 2. IRS-assisted bidirectional FD-MTC system.

Let  $\mathbf{h}^{(1)} = [h_1^{(1)} h_2^{(1)} \dots h_N^{(1)}]^T$  and  $\mathbf{h}^{(2)} = [h_1^{(2)} h_2^{(2)} \dots h_N^{(2)}]^T$ . The individual element in  $h_i^{(n)}$  is defined as,

$$h_i^{(n)} = |h_i^{(n)}| e^{j\theta_i^{(n)}}, i = 1, 2, \dots, N \ \& \ n = 1, 2 \tag{1}$$

The incident signal at the  $i^{th}$  element of IRS is given by

$$y_{IRS} = \sqrt{P_s} [h_i^{(1)} x_1 + h_i^{(2)} x_2] e^{-j\psi_i} \tag{2}$$

$\psi_i$  is the phase introduced by the IRS, which is the sum of the phases of the channel coefficients  $h_i^{(n)}, n = 1, 2$ . It is assumed that the phase of the channel coefficients  $h_i^{(n)}, n = 1, 2$  are perfectly known. In an ideal scenario, IRS is configured to choose the optimal (continuous) phase shift  $\psi_i, i = 1, 2, \dots, N$  at each element. In a practical scenario, complete phase compensation at IRS is not possible. Hence, it is configured as a discrete phase shifter of different phase levels: one-bit shifter  $b = 1$  ( $0, \pi$ ), two-bit shifter  $b = 2$  ( $0, \pi/2, \pi, 3\pi/2$ ) and three-bit shifter  $b = 3$  ( $0, \pi/4, \pi/2, 3\pi/4, \pi, 5\pi/4, 3\pi/2, 7\pi/4$ ). It is defined as

$$\psi_i = q_b(\theta_i^{(1)} + \theta_i^{(2)}), i = 1, 2, \dots, N, \tag{3}$$

where  $q_b(\cdot)$  is the quantized phase level of the discrete phase shifter. The received signal at IRS,  $y_{IRS}$  is reflected to source nodes  $S_1$  and  $S_2$  simultaneously through their reciprocity channels  $h_i^{(n)}, n = 1, 2$ , respectively. The received signals at the source nodes  $S_n, n = 1, 2$  are expressed as,

$$y_{s_n} = \sum_{i=1}^N h_i^{(n)} y_{IRS} + w_n + S I_n, n = 1, 2 \tag{4}$$

By substituting (3) in (4), the received signal at the source node  $S_1$  is rewritten as,

$$y_{s_1} = \sqrt{P_S} \sum_{i=1}^N |h_i^{(1)}|^2 e^{j(2\theta_i^{(1)} - \psi_i)} x_1 + \sqrt{P_S} \sum_{i=1}^N |h_i^{(1)}| |h_i^{(2)}| e^{j(\theta_i^{(1)} + \theta_i^{(2)} - \psi_i)} x_2 + w_1 + S I_1 \tag{5}$$

In the received signal at source node  $S_1$ , the first term consists of its own symbol  $x_1$  and the phase difference between  $h_i^{(1)}$  and IRS discrete phase shifter  $\psi_i$ . The random variable in the second term is defined as  $B = A e^{j(\theta_i^{(1)} + \theta_i^{(2)} - \psi_i)}$ , let  $A = \sum_{i=1}^N |h_i^{(1)}| |h_i^{(2)}|$ , it is the sum of the product of the magnitudes of  $h_i^{(1)}$  and  $h_i^{(2)} \forall i$ , and it follows a double Rayleigh distribution approximated by the first order term of the Laguerre series [33]. In the case of continuous phase shift at IRS, the phase term of  $\theta_i^{(1)}$  and  $\theta_i^{(2)}$  are completely compensated by IRS, and the corresponding distribution of random variable  $B = A$  is shown in Figure 3. In the case of discrete phase shift, the uncompensated phase term  $e^{j(\theta_i^{(1)} + \theta_i^{(2)} - \psi_i)}$  follows uniform distribution in  $(0, \pi)$  when  $b = 1$ ,  $(0, \pi/2, \pi, 3\pi/2)$  when  $b = 2$ , and  $(0, \pi/4, \pi/2, 3\pi/4, \pi, 5\pi/4, 3\pi/2, 7\pi/4)$  when  $b = 3$ . This discrete phase shifter affects the mean and variance of the random variable  $A$ . The Probability Density Function (PDF) for the random variable  $A$  is expressed as [33],

$$f_A(x) = \frac{x^\alpha}{\beta^{\alpha+1} \Gamma(\alpha + 1)} e^{-(x/\beta)} dx \tag{6}$$

where  $\alpha = \frac{K_1^2}{K_2} - 1$  and  $\beta = \frac{K_2}{K_1}$ . The parameters  $K_1$  and  $K_2$  are given by  $K_1 = E[A]$  and  $K_2 = 4Var[A]$ , respectively.

The mean and variance of the random variable  $A$  are expressed as [34],

$$E[A] = N \frac{\pi}{4}; \tag{7}$$

$$Var[A] = N \left( 1 - \frac{\pi^2}{16} \right) \tag{8}$$

By substituting the (7) and (8), the parameters  $\alpha$  and  $\beta$  are determined as

$$\alpha = \frac{N\pi^2}{16 - \pi^2} - 1 \tag{9}$$

$$\beta = \frac{16 - \pi^2}{2\pi} \tag{10}$$

The third and fourth terms in (5) are the additive white Gaussian noise (AWGN)  $w_n, n = 1, 2$  with variance  $N_0$  and SI  $SI_n, n = 1, 2$  with variance  $\sigma_w^2$ .

Similarly, the received signal at the source node  $S_2$  is expressed as,

$$y_{S_2} = \sqrt{P_s} \sum_{i=1}^N |h_i^{(2)}|^2 e^{j(2\theta_i^{(2)} - \psi_i)} x_2 + \sqrt{P_s} \sum_{i=1}^N |h_i^{(1)}| |h_i^{(2)}| e^{j(\theta_i^{(1)} + \theta_i^{(2)} - \psi_i)} x_1 + w_2 + SI_2 \quad (11)$$

In the case of the continuous phase shifter, (5) and (11) can be rewritten in terms of  $A$  as,

$$y_{S_1} = \sqrt{P_s} \sum_{i=1}^N |h_i^{(1)}|^2 e^{j(2\theta_i^{(1)} - \psi_i)} x_1 + \sqrt{P_s} A x_2 + w_1 + SI_1 \quad (12)$$

$$y_{S_2} = \sqrt{P_s} \sum_{i=1}^N |h_i^{(2)}|^2 e^{j(2\theta_i^{(2)} - \psi_i)} x_2 + \sqrt{P_s} A x_1 + w_2 + SI_2 \quad (13)$$

In the case of the discrete phase shifter, (5) and (11) can be rewritten in terms of  $B$  as,

$$q_{S_1} = \sqrt{P_s} \sum_{i=1}^N |h_i^{(1)}|^2 e^{j(2\theta_i^{(1)} - \psi_i)} x_1 + \sqrt{P_s} B x_2 + w_1 + SI_1 \quad (14)$$

$$q_{S_2} = \sqrt{P_s} \sum_{i=1}^N |h_i^{(2)}|^2 e^{j(2\theta_i^{(2)} - \psi_i)} x_2 + \sqrt{P_s} B x_1 + w_2 + SI_2 \quad (15)$$

The PDF of the ideal continuous and discrete phase shifter of 1-bit, 2-bits, and 3-bits are plotted using a histogram and it is shown in Figure 3. From Figure 3, it is clear that increasing the discrete phase shifter bit level shifts the mean and variance towards the ideal continuous phase shifter.

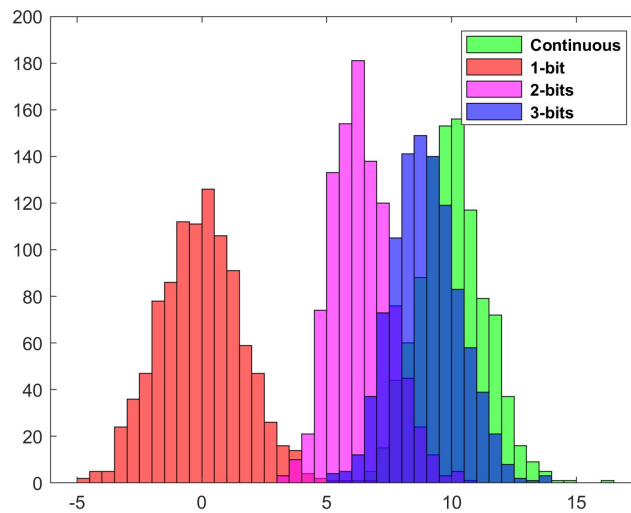


Figure 3. PDF of continuous and discrete phase shifter IRS.

### 3. Performance Analysis

#### 3.1. Outage Probability for IRS-Assisted Bidirectional FD-MTC System

The instantaneous SINR of the IRS-assisted bidirectional FD-MTC system, after compensation of the channel reciprocity, gains  $h_i^{(n)}, n = 1, 2$  at the source nodes  $S_1$  and  $S_2$ , is determined by using the Equations (12) and (13). It is given by,

$$X_{S_n} = \frac{P_s A^2}{N_0 + \sigma_w^2}, n = 1, 2 \quad (16)$$

The outage occurs at the source nodes  $S_1$  and  $S_2$  when it fails to decode the data successfully in the receiving mode and it is defined as [35],

$$P_{S_n}^{outage} = P(X_{S_n} \leq X_{TH}), n = 1, 2 \tag{17}$$

where  $X_{TH} = 2^{R_d} - 1$ ,  $R_d$  is the required data rate at both source nodes.  $P_{S_n}^{outage}$  is rewritten as,

$$P_{S_n}^{outage} = P\left(A \leq \sqrt{\frac{X_{TH}}{\rho_{S_n}}}\right), n = 1, 2 \tag{18}$$

where  $\rho_{S_n} = \frac{P_S}{N_0 + \sigma_w^2}$ , by substituting the PDF of  $A$  and solving using [36], the outage probability at the source nodes is determined as,

$$P_{S_n}^{outage} = \frac{\gamma\left(\frac{N\pi^2}{64-4\pi^2}, \frac{\pi}{16-\pi^2} \sqrt{\frac{X_{TH}}{\left(\frac{P_S}{N_0 + \sigma_w^2}\right)}}\right)}{\Gamma\left(\frac{N\pi^2}{64-4\pi^2}\right)}, n = 1, 2 \tag{19}$$

### 3.2. Bit Error Rate for IRS-Assisted Bidirectional FD-MTC System

Channel distribution  $A$  and the received SINR at two source nodes  $S_1$  and  $S_2$  determine the BER performance of the proposed system model. Since BPSK modulation is assumed, the average probability of error at both the source nodes  $S_1$  and  $S_2$  are given by,

$$P_{error}^{S_n} = \int_0^\infty Q(\sqrt{2\gamma_{S_n}}) f_{\Gamma_{S_n}}(\gamma_{S_n}) d\gamma_{S_n}, n = 1, 2 \tag{20}$$

where  $f_{\Gamma_{S_n}}(\gamma_{S_n})$  is the PDF of  $\gamma_{S_n}$ , it is obtained by taking the derivative of Cumulative Density Function (CDF)  $F_{\Gamma_{S_n}}(\gamma_{S_n})$ . By using (16), the CDF is defined as,

$$F_{\Gamma_{S_n}}(\gamma_{S_n}) = P\left[\frac{P_S A^2}{N_0 + \sigma_w^2} < \gamma_{S_n}\right], n = 1, 2 \tag{21}$$

Here  $A^2$  follows a Chi-square distribution with one degree of freedom. The CDF  $F_{\Gamma_{S_n}}(\gamma_{S_n})$  is expressed as,

$$F_{\Gamma_{S_n}}(\gamma_{S_n}) = \frac{1}{\sqrt{2}\Gamma\left(\frac{1}{2}\right)} \int_0^{\xi\gamma_{S_n}} a^{-\frac{1}{2}} e^{-\left(\frac{a}{2}\right)} da, n = 1, 2 \tag{22}$$

where  $\xi_n = \frac{1}{SNR}(a_{pt} + 1)$ ,  $a_{pt} = \frac{\sigma_w^2}{N_0}$ , Equation (22) is simplified as,

$$F_{\Gamma_{S_n}}(\gamma_{S_n}) = erf\left(\sqrt{\frac{\xi\gamma_{S_n}}{2}}\right), n = 1, 2 \tag{23}$$

The corresponding PDF  $f_{\Gamma_{S_n}}(\gamma_{S_n})$  is derived as,

$$f_{\Gamma_{S_n}}(\gamma_{S_n}) = \frac{1}{\sqrt{2\pi\gamma_{S_n}}} \sqrt{\frac{(a_{pt} + 1)}{SNR}} exp\left(-\frac{\xi\gamma_{S_n}}{2}\right), n = 1, 2 \tag{24}$$

By using (24), (20) can be rewritten as,

$$P_{error}^{S_n} = \frac{\sqrt{\xi_n}}{\sqrt{2\pi\gamma_{S_n}}} \int_0^\infty Q(\sqrt{2\gamma_{S_n}}) exp\left(-\frac{\xi\gamma_{S_n}}{2}\right) d\gamma_{S_n}, n = 1, 2 \tag{25}$$

Using the Q-function approximation  $Q(x) = \frac{1}{2} - \frac{1}{2} \operatorname{erf}\left(\frac{x}{\sqrt{2}}\right)$ , the average probability of error expression is re-written as,

$$P_{error}^{S_n} = \frac{\sqrt{\xi_n}}{2\sqrt{2\pi}} \int_0^\infty \left[ \frac{\exp\left(-\frac{\xi_n \gamma_{S_n}}{2}\right)}{\sqrt{\gamma_{S_n}}} - \operatorname{erf}\left(\sqrt{\gamma_{S_n}}\right) \frac{\exp\left(-\frac{\xi_n \gamma_{S_n}}{2}\right)}{\sqrt{\gamma_{S_n}}} \right] d\gamma_{S_n}, n = 1, 2 \quad (26)$$

The probability of error at the IRS-assisted bidirectional FD-MTC system is determined by solving (26), using [36],

$$P_{error}^{S_n} = \frac{1}{2\sqrt{2\pi}} \sqrt{\frac{a_{pt} + 1}{SNR}} \left[ \frac{2\pi}{\xi_n} - \frac{2}{\xi \sqrt{\frac{\xi_n}{2} + 1}} \right], n = 1, 2 \quad (27)$$

### 3.3. Achievable Rate for IRS-Assisted Bidirectional FD-MTC System

To find the best location of IRS to achieve better transmission for a proposed IRS-assisted bidirectional FD-MTC system, an achievable rate is calculated by placing IRS at a different distance from the machine as shown in Figure 4. The achievable rate is determined by the channel capacity, which is the maximum information rate that can be transmitted over a channel with an arbitrarily small error probability. The achievable rate can be lower than the channel capacity if the transmitted signal is not optimized for the channel conditions, or if the receiver does not have sufficient processing power to decode the signal. It is expressed as [37],

$$P_r = N^2 \frac{P_t \pi^2 \rho_h^2 \rho_g^2}{16} \quad (28)$$

where  $P_r$  is the received power, and  $P_t$  is the transmitted power. The scenario assumes i.i.d. Rayleigh fading, where the average power of each entry in the fading vectors  $h_i^{(1)}$  and  $h_i^{(2)}$  is denoted by  $\rho_h^2$  and  $\rho_g^2$ , respectively. It is assumed that the average power of the fading vectors as  $\rho_h^2 = C_0 d_1^{(-\zeta)}$ ,  $\rho_g^2 = C_0 d_2^{(-\zeta)}$ , where  $d_1, d_2$  is the corresponding link distance in meters (m),  $C_0$  is the path loss at reference distance and  $\zeta$  is the path loss exponent.

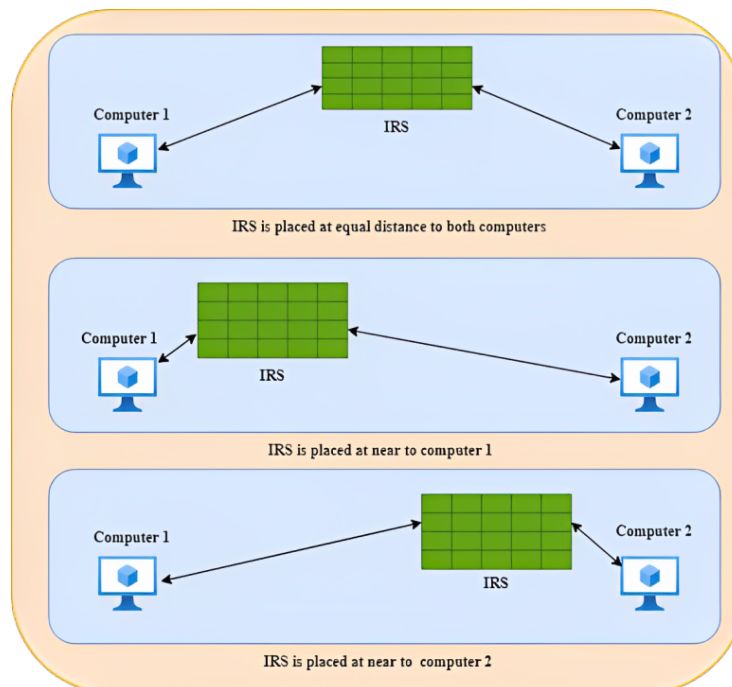


Figure 4. Various locations of IRS in bidirectional FD-MTC system.

#### 4. Results and Discussion

The simulations are carried out in the MATLAB R2022b environment and the simulation parameters considered for the performance analysis of the proposed IRS-assisted bidirectional FD-MTC system are shown in Table 1. In the proposed IRS-assisted bidirectional FD-MTC system, it is assumed that IRS is placed halfway between the two source nodes  $S_1$  and  $S_2$ ; hence, both outage probability and BER performance analysis behave similarly for both source nodes  $S_n, n = 1, 2$ .

**Table 1.** Simulation parameters.

Parameter	Values
$N$ (number of meta surface elements in IRS)	16, 32, 64
Self-Interference (SI)	5 dB, 10 dB, 15 dB, 20 dB
SNR in dB	−30 to 10
Required data rate	2 bps/Hz
MC Simulation	5000
Power transmitted	50 mW
$C_0$	−30 dB
The path loss exponent $\zeta$	2
Distance between IRS and $S_1$ in meters	Near case: 10, 20, 30 Far case: 90, 80, 70 Equal case: 50
Distance between IRS and $S_2$ in meters	Near case: 10, 20, 30 Far case: 90, 80, 70 Equal case: 50
Phases of 1-bit discrete phase shifter	$0, \pi$
Phases of 2-bits discrete phase shifter	$0, \pi/2, \pi, 3\pi/2$
Phases of 3-bits discrete phase shifter	$0, \pi/4, \pi/2, 3\pi/4, \pi, 5\pi/4, 3\pi/2, 7\pi/4$
Target outage probability	$10^{-3}$
Target BER	$10^{-6}$
Noise variance ( $N_0$ )	Normalized to 1

The MC simulations of the outage performance for the IRS-assisted bidirectional FD-MTC system with a different number of reflecting elements ( $N = 16, 32, 64$ ) in the Rayleigh fading environment is shown in Figure 5 and it is verified using the derived analytical expression. For the target outage probability value of  $10^{-3}$  in Figure 5, there is  $\approx 6$  dB improvement in the proposed system model by doubling the number of meta surface elements  $N$  in IRS. From Equation (19), it is inferred that, if the ratio  $\frac{X_{TH}}{\rho_{S_n}}$  is held constant, the outage probability decreases with respect to the number of meta surface elements  $N$  in IRS. Similarly, if the value of  $N$  is fixed, an increase in the ratio of  $\frac{X_{TH}}{\rho_{S_n}}$  causes a decrease in the outage probability. Therefore, increasing the  $\frac{X_{TH}}{\rho_{S_n}}$  leads to an improvement in the outage performance for a fixed value of meta surface elements  $N$ .

The comparison of the outage probability for IRS-assisted bidirectional FD-MTC system with HD-MTC system with various values of meta surface reflecting elements ( $N = 16, 32$ ) and  $SI = 5$  dB, 10 dB, 15 dB, and 20 dB are shown in Figures 6–9. From Figures 6–9, it is observed that, when the  $SI$  at the source node is increased from 5 dB with an incremental step size of 5 dB up to 15 dB, the outage probability value of IRS-assisted bidirectional FD-MTC system increases and gets closer to the performance of HD-MTC system. For 20 dB  $SI$ , the outage probability value degrades more than the HD-MTC system.

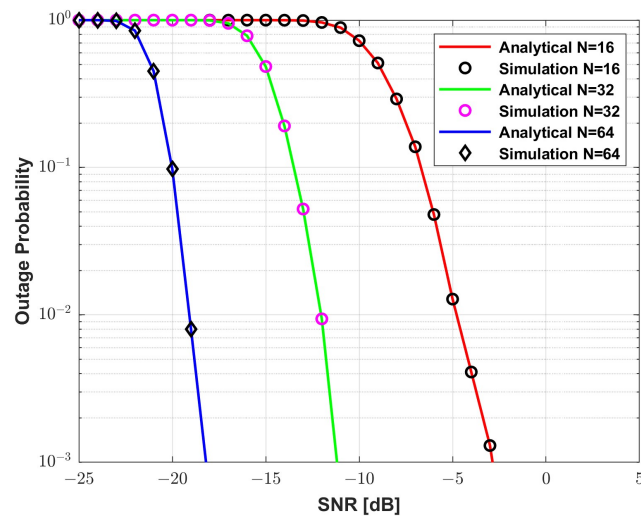


Figure 5. Outage probability for IRS-assisted bidirectional FD-MTC system.

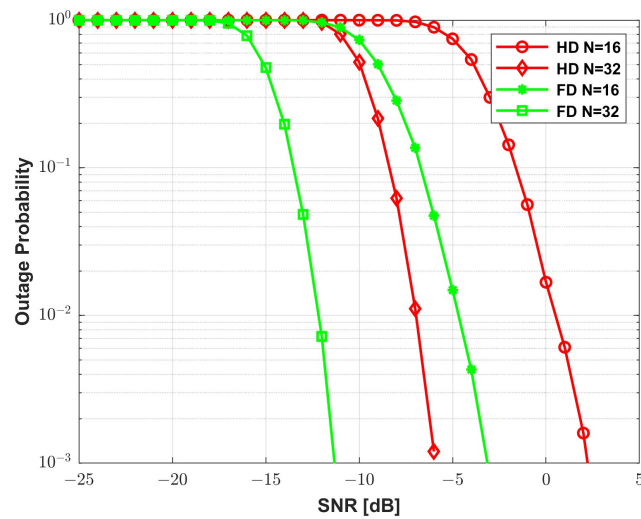


Figure 6. Outage probability of IRS-assisted bidirectional HD vs. FD MTC system at SI = 5 dB.

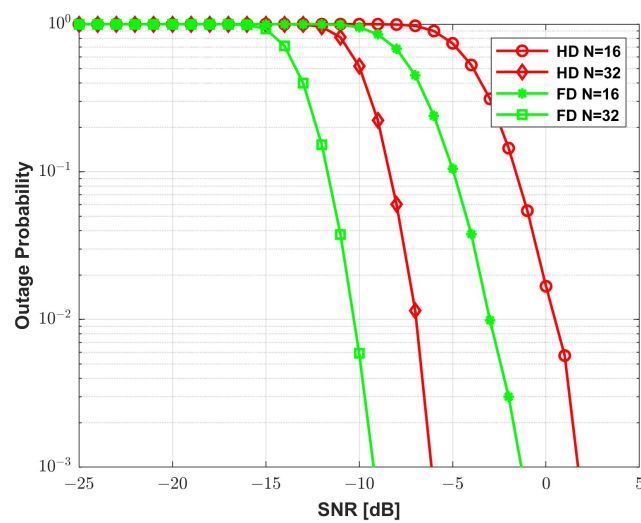


Figure 7. Outage probability of IRS-assisted bidirectional HD vs. FD MTC system at SI = 10 dB.

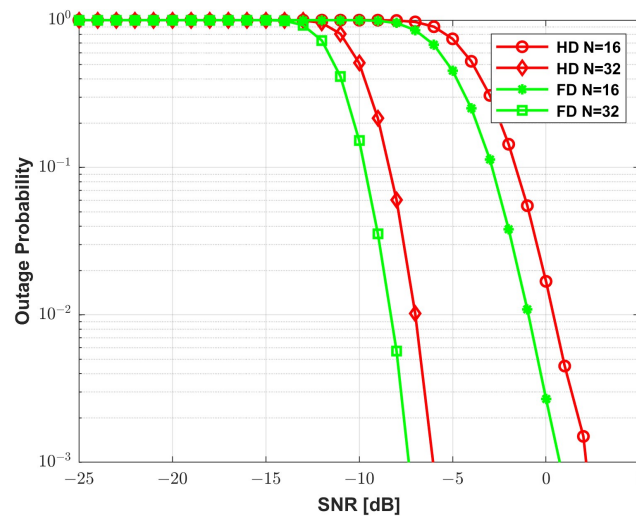


Figure 8. Outage probability of IRS-assisted bidirectional HD vs. FD MTC system at SI = 15 dB.

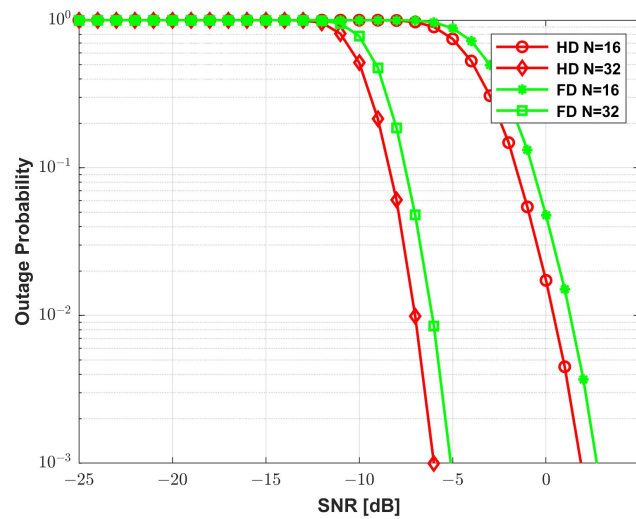


Figure 9. Outage probability of IRS-assisted bidirectional HD vs. FD MTC system at SI = 20 dB.

The BER performance of the IRS-assisted bidirectional FD-MTC system with different numbers of meta surface reflecting elements ( $N = 16, 32, 64$ ) in a Rayleigh fading environment is shown in Figure 10. From Equation (27), it is inferred that, if the ratio  $a_{pt} = \frac{\sigma_w^2}{N_0}$ , is held constant, the BER decreases with respect to the number of meta surface elements  $N$  in IRS. Similarly, if the value of  $N$  and  $a_{pt} = \frac{\sigma_w^2}{N_0}$  are fixed, increasing  $\zeta_n = \frac{1}{SNR}(a_{pt} + 1)$  leads to an improvement in the BER performance. For the target BER value of  $10^{-6}$ , there is  $\approx 8$  dB improvement in the proposed system model by doubling the number of meta surface elements  $N$  in IRS.

The comparison of BER performance of ideal continuous and discrete phase shifters of 1-bit, 2-bits, and 3-bits for  $N = 32$  is shown in Figure 11. It is inferred that, the 1-bit shifter at IRS results in poor performance for a bidirectional FD-MTC system. By increasing the bit level of the discrete phase shifter at IRS, the BER performance improves and it approaches the ideal continuous phase shifter at IRS.

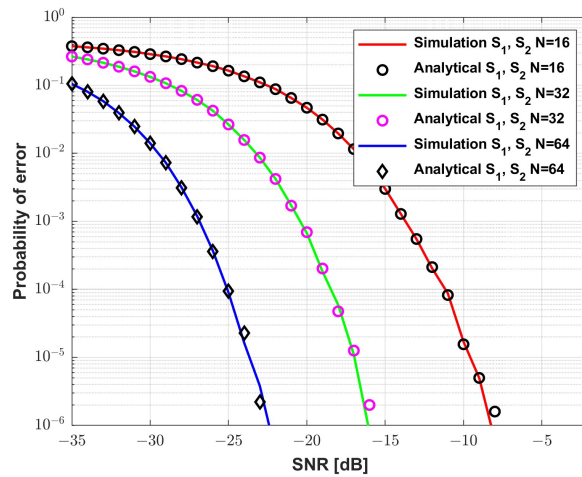


Figure 10. BER for IRS-assisted bidirectional FD-MTC system.

The comparison of outage performance of ideal continuous and discrete phase shifters of 1-bit, 2-bits, and 3-bits for  $N = 32$  is shown in Figure 12. From the PDF plot of the discrete phase shifter in Figure 3 and the outage performance in Figure 12, the variance of the discrete phase shifter for the different bit level  $b$  is obtained as,

$$Var[b] = \eta 2^b \tag{29}$$

where  $\eta$  is the difference between the SNR-dB of the  $b$ -level phase shifter and the SNR-dB of the ideal continuous phase shifter at a particular outage probability value. Also, increasing the bit level of the discrete phase shifter at IRS improves the outage performance and it approaches the ideal continuous phase shifter at IRS. As seen in Figures 11 and 12, a 3-bit discrete phase shifter requires just 1 dB more than an ideal continuous phase shifter at IRS to achieve the desired BER and outage.

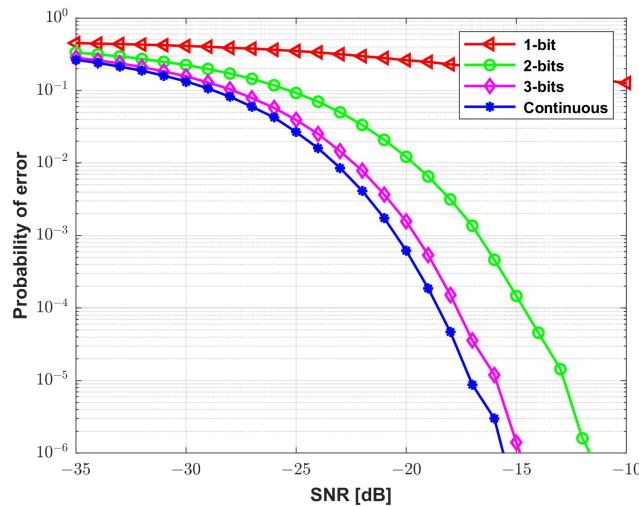
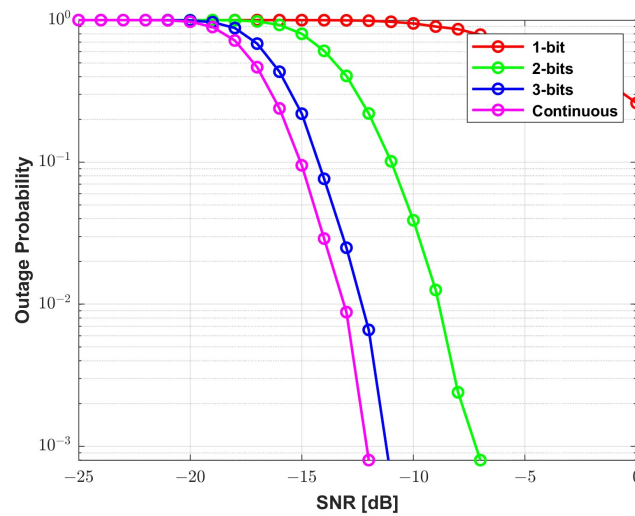
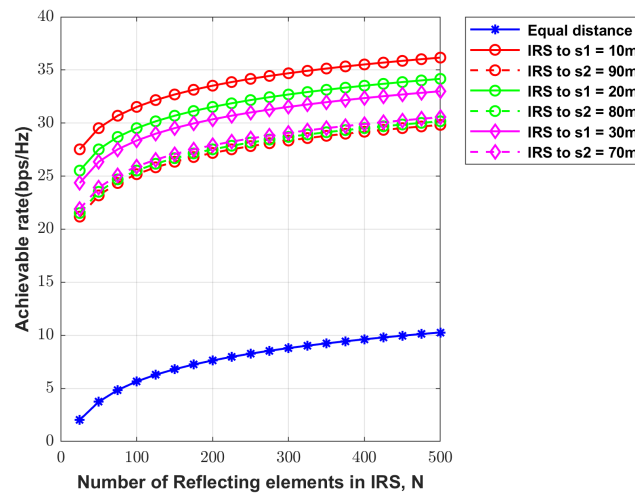


Figure 11. BER for IRS-assisted bidirectional FD-MTC system in continuous and discrete phase shifter.

The achievable rate performance of various locations of the IRS-assisted bidirectional FD-MTC system is shown in Figure 13. It is inferred, when the IRS is placed closer to any of the source nodes, the achievable rate for that particular source node is better than the source node which is far away from the IRS.



**Figure 12.** Outage probability for IRS-assisted bidirectional FD-MTC system with continuous and discrete phase shifter.



**Figure 13.** Achievable rate for IRS-assisted bidirectional FD-MTC system.

**5. Conclusions**

The 5G and B5G networks use high-frequency waves that can be easily blocked by physical objects and environmental factors, making it difficult for data transfer over long distances. To overcome this challenge, the IRS mechanism has been proposed as a solution for achieving reliable 5G and B5G communication. In this paper, the performance of an IRS-assisted MTC bidirectional system in terms of outage probability, BER, and the achievable rate is analyzed in FD mode. The outage performance of the IRS-assisted bidirectional communication system in FD mode has an SNR improvement of  $\approx 6$  dB compared to the IRS-assisted bidirectional communication system in HD mode. Additionally, the BER performance of the IRS-assisted bidirectional communication system in FD mode has an SNR improvement of  $\approx 8$  dB as the number of meta surface reflecting elements doubles in the IRS. Further, this study investigates the impact of using a discrete phase shifter on bidirectional communication systems with an IRS and evaluates the outage BER performance of the system. The study considers three different levels of the discrete phase shifter, namely the 1-bit shifter  $(0, \pi)$ , 2-bit shifter  $(0, \pi/2, \pi, 3\pi/2)$ , and for the 3-bit shifter  $(0, \pi/4, \pi/2, 3\pi/4, \pi, 5\pi/4, 3\pi/2, 7\pi/4)$ , and compares the system’s error degradation with the ideal continuous phase shifter of IRS. The results indicate that the presence of residue degrades the system performance when using a 1-bit phase shifter while increasing the number of phase shifters to 2-bits and 3-bits and so on improves the system’s performance compared to the 1-bit phase shifter. IRS located near the source node provides a better achievable

rate than the halfway between the two source nodes of the bidirectional FD-MTC system. In future work, the analysis of the IRS-assisted bidirectional FD-MTC system can be carried out for spatial correlation and mutual coupling at IRS. Theoretical results in this manuscript can be extended to multiple source nodes with more than two antennas, with appropriate antenna selection technique and number of IRS at appropriate places. This is being carried out as future work.

**Author Contributions:** P.G.S.V. and S.J.T. were responsible for the conceptualization of the topic; article gathering and sorting were carried out by P.G.S.V., S.R., R.P., S.J.T., V.B.K. and A.L.I.; manuscript writing and original drafting and formal analysis were carried out by P.G.S.V., S.R., R.P., S.J.T., V.B.K. and A.L.I. All authors have read and agreed to the published version of the manuscript.

**Funding:** The work of Agbotiname Lucky Imoize was supported in part by the Nigerian Petroleum Technology Development Fund (PTDF) and in part by the German Academic Exchange Service (DAAD) through the Nigerian–German Postgraduate Program under grant 57473408.

**Institutional Review Board Statement:** Not applicable.

**Informed Consent Statement:** Not applicable.

**Data Availability Statement:** All data are available from the corresponding author with reasonable request.

**Conflicts of Interest:** The authors declare no conflict of interest.

## Abbreviations

The following abbreviations are used in this manuscript:

MTC	Machine Type Communication
M2M	Machine-to-Machine
IRS	Intelligent Reflecting Surface
FD	Full Duplex
HD	Half Duplex
BER	Bit Error Rate
SNR	Signal-to-Noise Ratio
mm	Millimetre
IoT	Internet of Things
URLLC	Ultra-Reliable Low-Latency Communications
STAR	Simultaneous Transmission And Reflection
UL	Uplink
DL	Downlink
PDF	Probability Density Function
MC	Monte Carlo
BLER	Block Error Rate
SI	Self Interference
BS	Base Station
D2D	Device-to-Device
SINR	Signal-to-Interference Noise Ratio
MIMO	Multiple Input Multiple Output
LoS	Line of Sight
BPSK	Binary Phase Shift Keying
AWGN	Additive White Gaussian Noise
CDF	Cumulative Density Function
IBFD	In-Band Full Duplex

## References

1. Chowdhury, M.Z.; Shahjalal, M.; Ahmed, S.; Jang, Y.M. 6G wireless communication systems: Applications, requirements, technologies, challenges, and research directions. *IEEE Open J. Commun. Soc.* **2020**, *1*, 957–975. [\[CrossRef\]](#)
2. De Alwis, C.; Kalla, A.; Pham, Q.V.; Kumar, P.; Dev, K.; Hwang, W.J.; Liyanage, M. Survey on 6G frontiers: Trends, applications, requirements, technologies and future research. *IEEE Open J. Commun. Soc.* **2021**, *2*, 836–886. [\[CrossRef\]](#)
3. Okogbaa, F.C.; Ahmed, Q.Z.; Khan, F.A.; Abbas, W.B.; Che, F.; Zaidi, S.A.R.; Alade, T. Design and Application of Intelligent Reflecting Surface (IRS) for Beyond 5G Wireless Networks: A Review. *Sensors* **2022**, *22*, 2436. [\[CrossRef\]](#) [\[PubMed\]](#)
4. Jain, P.; Gupta, A.; Kumar, N.; Guizani, M. Dynamic and Efficient Spectrum Utilization for 6G With THz, mmWave, and RF Band. *IEEE Trans. Veh. Technol.* **2023**, *72*, 3264–3273. [\[CrossRef\]](#)
5. Du, C.; Xie, L.; Xing, Z.; An, J.; Zhang, Z. Self-Interference Cancellation-Based Workload-Driven Duplex-Model Selection in Machine-Type Communication Networks. *IEEE Internet Things J.* **2022**, *9*, 20189–20202. [\[CrossRef\]](#)
6. Björnson, E.; Özdogan, Ö.; Larsson, E.G. Intelligent Reflecting Surface Versus Decode-and-Forward: How Large Surfaces are Needed to Beat Relaying? *IEEE Wirel. Commun. Lett.* **2020**, *9*, 244–248. [\[CrossRef\]](#)
7. Thirumavalavan, V.C.; Ruppia Hariharan, A.B.; Thiruvengadam S.J. BER analysis of tightly packed planar RIS system using the level of spatial correlation and discrete phase shifter. *Trans. Emerg. Telecommun. Technol.* **2022**, *33*, e4596. [\[CrossRef\]](#)
8. Jamshed, M.A.; Ali, K.; Abbasi, Q.H.; Imran, M.A.; Ur-Rehman, M. Challenges, applications and future of wireless sensors in Internet of Things: A review. *IEEE Sens. J.* **2022**, *22*, 5482–5494. [\[CrossRef\]](#)
9. Noor-A-Rahim, M.; Firyaguna, F.; John, J.; Khyam, M.O.; Pesch, D.; Armstrong, E.; Poor, H.V. Toward Industry 5.0: Intelligent Reflecting Surface in Smart Manufacturing. *IEEE Commun. Mag.* **2022**, *60*, 72–78. [\[CrossRef\]](#)
10. Ucar-Gul, M.; Namdar, M.; Basgumus, A. Performance analysis of two-way AF relaying system with the presence of hardware impairments over Nakagami-m fading channels. *IET Commun.* **2020**, *14*, 2618–2627. [\[CrossRef\]](#)
11. Wang, Y.; Guan, P.; Yu, H.; Zhao, Y. Transmit power optimization of simultaneous transmission and reflection RIS assisted Full-Duplex communications. *IEEE Access* **2022**, *10*, 61192–61200. [\[CrossRef\]](#)
12. Karim, F.; Singh, S.K.; Singh, K.; Flanagan, M.F. STAR-RIS aided Full Duplex Communication System: Performance Analysis. In Proceedings of the GLOBECOM 2022–2022 IEEE Global Communications Conference, Rio de Janeiro, Brazil, 4–8 December 2022; pp. 3114–3119.
13. Karim, F.; Hazarika, B.; Singh, S.K.; Singh, K. A performance analysis for multi-RIS-assisted full duplex wireless communication system. In Proceedings of the ICASSP 2022–2022 IEEE International Conference on Acoustics, Speech and Signal Processing (ICASSP), Singapore, 23–27 May 2022; pp. 5313–5317.
14. Singh, S.K.; Agrawal, K.; Singh, K.; Li, C.P.; Ding, Z. A NOMA-enabled Hybrid RIS-UAV-aided Full-Duplex Communication System. In Proceedings of the 2022 Joint European Conference on Networks and Communications & 6G Summit (EuCNC/6G Summit), Grenoble, France, 7–10 June 2022; pp. 529–534.
15. Guan, P.; Wang, Y.; Yu, H.; Zhao, Y. Energy efficiency maximisation for STAR-RIS assisted full-duplex communications. *IET Commun.* **2023**, *17*, 603–613. [\[CrossRef\]](#)
16. Wang, Y.; Guan, P.; Yu, H.; Zhao, Y. Energy efficiency of full-duplex communication system assisted by reconfigurable intelligent surface. *IET Commun.* **2023**, *17*, 478–488. [\[CrossRef\]](#)
17. Liu, X.; Xu, B.; Wang, X.; Zheng, K.; Chi, K.; Tian, X. Impacts of Sensing Energy and Data Availability on Throughput of Energy Harvesting Cognitive Radio Networks. *IEEE Trans. Veh. Technol.* **2022**, *72*, 747–759. [\[CrossRef\]](#)
18. Zheng, K.; Jia, X.; Chi, K.; Liu, X. DDPG-Based Joint Time and Energy Management in Ambient Backscatter-Assisted Hybrid Underlay CRNs. *IEEE Trans. Commun.* **2023**, *71*, 441–456. [\[CrossRef\]](#)
19. Dhok, S.; Raut, P.; Sharma, P.K.; Singh, K.; Li, C.P. Non-linear energy harvesting in RIS-assisted URLLC networks for industry automation. *IEEE Trans. Commun.* **2021**, *69*, 7761–7774. [\[CrossRef\]](#)
20. Peng, Z.; Zhang, Z.; Pan, C.; Li, L.; Swindlehurst, A.L. Multiuser full-duplex two-way communications via intelligent reflecting surface. *IEEE Trans. Signal Process.* **2021**, *69*, 837–851. [\[CrossRef\]](#)
21. Guan, P.; Wang, Y.; Yu, H.; Zhao, Y. Joint beamforming optimization for RIS-aided full-duplex communication. *IEEE Wirel. Commun. Lett.* **2022**, *11*, 1629–1633. [\[CrossRef\]](#)
22. Singh, K.; Wang, P.C.; Biswas, S.; Singh, S.K.; Mumtaz, S.; Li, C.P. Joint Active and Passive Beamforming Design for RIS-Aided IBFD IoT Communications: QoS and Power Efficiency Considerations. *IEEE Trans. Consum. Electron.* **2022**, *69*, 170–182. [\[CrossRef\]](#)
23. Peng, Z.; Zhang, Z.; Kong, L.; Pan, C.; Li, L.; Wang, J. Deep reinforcement learning for ris-aided multiuser full-duplex secure communications with hardware impairments. *IEEE Internet Things J.* **2022**, *9*, 21121–21135. [\[CrossRef\]](#)
24. Alakoca, H.; Namdar, M.; Aldirmaz-Colak, S.; Basaran, M.; Basgumus, A.; Durak-Ata, L.; Yanikomeroğlu, H. Metasurface Manipulation Attacks: Potential Security Threats of RIS-Aided 6G Communications. *IEEE Commun. Mag.* **2023**, *61*, 24–30. [\[CrossRef\]](#)
25. Yaxuan, L.; Haitao, Z.; Yiyang, N.; Hui, Z.; Fan, Y.; Hongbo, Z. Transmission mode switching for relay/RIS assisted device-to-device communication networks. In Proceedings of the IEEE/CIC International Conference on Communications in China (ICCC Workshops), Xiamen, China, 28–30 July 2021; pp. 133–136.
26. Gang, Y.; Yating, L.; Ying-Chang, L.; Olav, T.; Gongpu, W.; Xing, Z. Reconfigurable Intelligent Surface Empowered Device-to-Device Communication Underlying Cellular Networks. *IEEE Trans. Commun.* **2021**, *69*, 7790–7805.

27. Chen, Y.; Ai, B.; Zhang, H.; Niu, Y.; Song, L.; Han, Z.; Vincent Poor, H. Reconfigurable Intelligent Surface Assisted Device-to-Device Communications. *IEEE Trans. Wirel. Commun.* **2021**, *20*, 2792–2804. [[CrossRef](#)]
28. Lu, Y.; Hao, M.; Mackenzie, R. Reconfigurable intelligent surface based hybrid precoding for THz communications. *Intell. Conver. Netw.* **2022**, *3*, 103–118. [[CrossRef](#)]
29. Xiong, J.; You, L.; Ng, D.W.K.; Yuen, C.; Wang, W.; Gao, X. Energy efficiency and spectral efficiency tradeoff in RIS-aided multiuser MIMO uplink systems. In Proceedings of the GLOBECOM 2020–2020 IEEE Global Communications Conference, Taipei, Taiwan, 7–11 December 2020; pp. 1–6.
30. You, L.; Xiong, J.; Ng, D.W. K.; Yuen, C.; Wang, W.; Gao, X. Energy efficiency and spectral efficiency tradeoff in RIS-aided multiuser MIMO uplink transmission. *IEEE Trans. Signal Process.* **2020**, *69*, 1407–1421. [[CrossRef](#)]
31. Wu, Q.; Zhang, R. Beamforming optimization for wireless network aided by intelligent reflecting surface with discrete phase shifts. *IEEE Trans. Commun.* **2019**, *68*, 1838–1851. [[CrossRef](#)]
32. Dai, L.; Wang, B.; Wang, M.; Yang, X.; Tan, J.; Bi, S.; Hanzo, L. Reconfigurable intelligent surface-based wireless communications: Antenna design, prototyping, and experimental results. *IEEE Access* **2020**, *8*, 45913–45923. [[CrossRef](#)]
33. Primak, S.; Kontorovich, V.; Lyandres, V. *Stochastic Methods and Their Applications to Communications Stochastic Differential Equations Approach*; John Wiley & Sons, Ltd.: Hoboken, NJ, USA, 2004.
34. Basar, E.; di Renzo, M.; de Rosny, J.; Debbah, M.; Alouini, M.S.; Zhang, R. Wireless Communications Through Reconfigurable Intelligent Surfaces. *IEEE Access* **2019**, *7*, 116753–116773. [[CrossRef](#)]
35. Jadhav, H.K.; Kumaravelu, V.B. Blind RIS Aided Ordered NOMA: Design, Probability of Outage Analysis and Transmit Power Optimization. *Symmetry* **2022**, *14*, 2266. [[CrossRef](#)]
36. Table of Integrals. Available online: <https://link.springer.com/content/pdf/bbm:978-1-4612-1520-2/1> (accessed on 3 April 2023).
37. Qingqing, W.; Shuowen, Z.; Beixiong, Z.; Changsheng, Y.; Rui, Z. Intelligent Reflecting Surface-Aided Wireless Communications: A Tutorial. *IEEE Trans. Commun.* **2021**, *69*, 3313–3351.

**Disclaimer/Publisher’s Note:** The statements, opinions and data contained in all publications are solely those of the individual author(s) and contributor(s) and not of MDPI and/or the editor(s). MDPI and/or the editor(s) disclaim responsibility for any injury to people or property resulting from any ideas, methods, instructions or products referred to in the content.